SAND2012-2369 C

SAND2012-2369C

Bistatic SAR imaging of the lunar surface using the Arecibo observatory transmitter and the lunar reconnaissance orbiter receiver

Daniel E. Wahl[a], David Yocky[a], Ben Bussey[b], Charles Jakowatz, Jr.[a]
[a]Sandia National Laboratories PO Box 5800 Albuquerque, NM 87185-1207 ; [b]Johns Hopkins Applied Physics Lab

ABSTRACT

Polarimetric bistatic SAR imaging of the lunar surface may allow detection of ice at the bottom of certain craters. We have employed the Arecibo Observatory radar transmitter and the mini-RF radar aboard the National Aeronautics and Space Administration (NASA) Lunar Reconnaissance Orbiter (LRO) as a receiver to collect such bistatic data of the lunar surface. In this paper, we demonstrate the ability to form bistatic polarimetric imagery with spatial resolution on the order of 50m, and to create polarimetric maps that could potentially reveal the presence of deep crater ice. We discuss the details of the signal processing techniques that are required to allow these products to be formed.

Keywords: Bistatic SAR imaging, polarimetry, lunar ice detection

1. INTRODUCTION

The question of the existence of ice at the bottom of certain lunar craters that are never illuminated by the sun has been one of longstanding interest [1],[2],[3]. One possibility for such lunar ice detection is through the use of monostatic SAR imaging using polarimetric data [4],[5]. The NASA system known as the Lunar Reconnaissance Orbiter (LRO) was launched with hopes of utilizing monostatic synthetic aperture radar (SAR) polarimetric imagery to help answer this question. Unfortunately, the LRO transmitter failed in December 2010, so that monostatic SAR imaging was rendered impossible. An interesting alternative was suggested, however. The proposal was to obtain bistatic SAR polarimetric imagery using the Arecibo Observatory transmitter and the LRO radar as a receiver. In this paper we describe how such bistatic data are collected and processed into appropriate imagery products that can potentially help answer the question of lunar ice existence.

2. DATA COLLECTIONS

The Arecibo Observatory radio telescope is a 305-m dish transmitter/receiver located on the island of Puerto Rico. It illuminated a portion of the lunar surface with a 35.5W peak power, circularly polarized, S-band (2.3975 GHz) chirped signal on April 6, 2011. The parameters of the transmitted pulse are shown in Table 1.

Table 1. Arecibo transmitted RADAR signal parameters

Waveform Parameters	*Value*
Pulse length	100 μs
Pulse repetition interval	500 μs
Chirp start frequency	2.3792 GHz
Chirp rate	0.016 MHz/μs

Updated 1 March 2012

Mini-RF, the radar receiver onboard the LRO, receives two linear polarizations, namely horizontal and vertical polarization components. For this test, the LRO Mini-RF receiver was operated in continuous mode and the received signal was digitized with in-phase and quadrature channels using three bits at a rate of 2.0833 MHz.

There were three primary kinds of returns identified in the data: 1) direct-path signals that are propagated directly from Arecibo to the LRO; 2) specular signals that bounce off the surface of the moon at the specular point; and 3) ground-bounce signals that correspond to signals that are reflected from the surface of the moon where the illuminating antenna pattern from Arecibo and the LRO receive antenna pattern intersect. Ground-bounce singles of the third kind are the ones that contain the data used for image formation. The direct-path signals of the first kind were used to synchronize the timing and phasing necessary to produce focused imagery. The direct-path signals and the specular return signals (second kind) came in through a back side-lobe of the antenna.

3. PREPROCESSING OF BISTATIC DATA

Preprocessing the raw data consists of all the steps required to decimate the original continuously recorded data into the normal motion-compensated pulsed data that is required for any strip-map image formation algorithm. The first step was to form a range-compressed phase history data set. The original data was divided into intervals commensurate with the pulse-repetition-interval (PRI) and compressed using the known transmitted chirp. The top graphic of Figure 1 shows a portion of these range-compressed data. The magnitude of these data was incoherently summed along pulses producing a one-dimensional signal shown in the bottom graphic of Figure 1. Examination of this signal reveals the three kinds of returns described in Section 2., namely direct path, specular, and ground bounce.

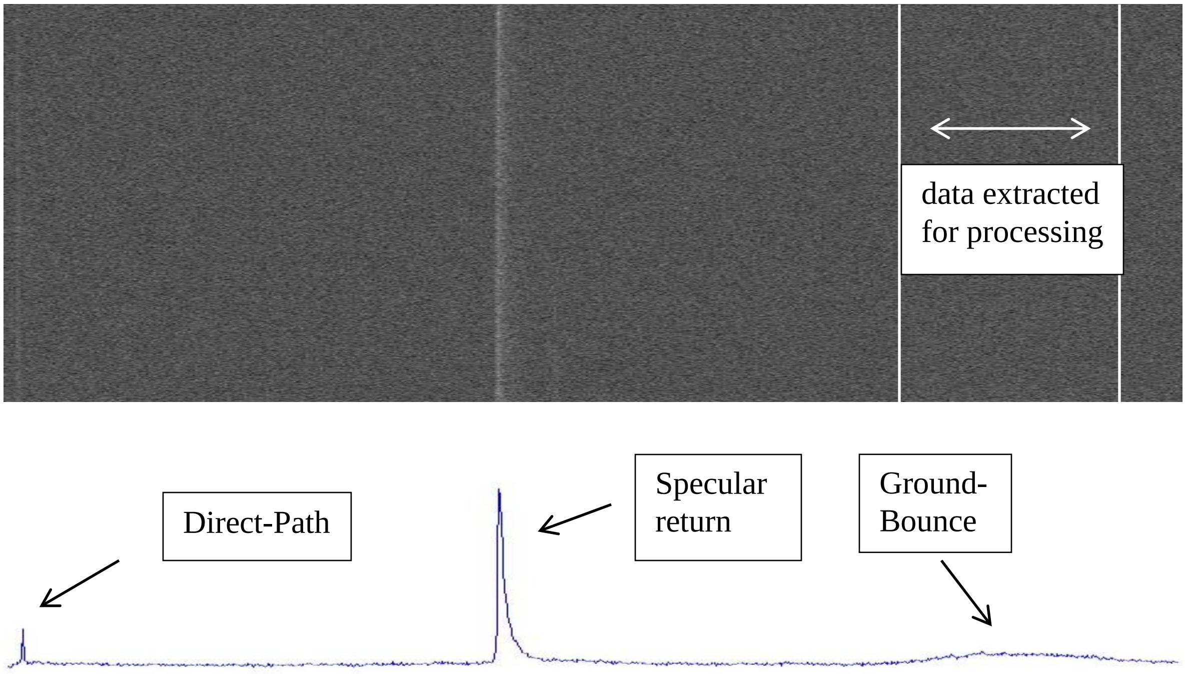

Figure 1. Top: A portion of the range-compressed data artificially divided using the given pulse-repetition-interval; Bottom: Incoherent sum (along pulses) of the range-compressed data.

The location and the phase of each direct-path pulse was carefully measured and utilized along with the geometry of the collect to extract and phase-compensate each range-compressed pulse. The region of data extracted and phase compensated is shown in the top graphic of Figure 1 and is calculated from the location of the direct-path, the geometry of the collect and the beam size on the surface of the moon. The extracted and phase-compensated pulses were then used by the beamforming algorithm described below to form the image.

4. METHODOLOGY FOR BISTATIC IMAGE FORMATION

In previous papers the authors have suggested the utility of bistatic SAR image formation via a beamforming or backprojection algorithm [6]. We employed this technique on the lunar data described in Section 2. Figure 2 shows the horizontal polarization image reconstructed via backprojection. It is as 400-km by 40-km swath of the moon. Left-to-right is north-to-south. Figure 3 shows the vertical polarization image using the same backprojection image formation code.

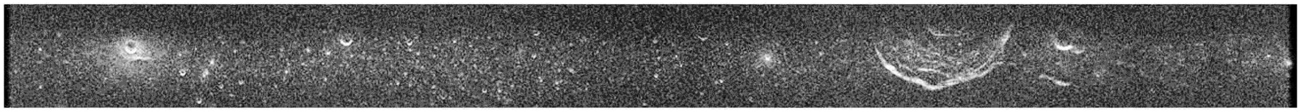

Figure 2. Horizontal polarization bistatic SAR image for a 400-km north-to-south swath of the moon. The large crater on the right is Hansteen crater at 11° 30' 32'' S, 52° 00' 09'' W.

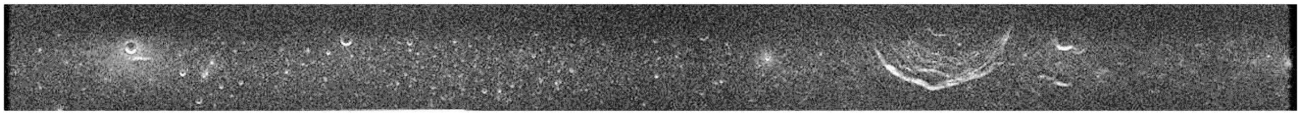

Figure 3. Vertical polarization bistatic SAR image for collection described above.

5. POLARIZATION PROCESSING AND STOKES PARAMETERS

The Stokes parameters of the scattered lunar field can be expressed in terms of the complex-valued dual-polarization-channels received by mini-RF on LRO as follows [7]:

$$S_1 = \left\langle |E_H|^2 + |E_V|^2 \right\rangle \qquad S_2 = \left\langle |E_H|^2 - |E_V|^2 \right\rangle \qquad S_3 = 2\,\mathrm{Re}\left\langle E_H E_V^* \right\rangle \qquad S_4 = 2\,\mathrm{Im}\left\langle E_H E_V^* \right\rangle$$

where E denotes the complex linear-polarization value, * denotes complex conjugate, < . . . > denotes ensemble averaging, and Re and Im denote the real or the imaginary value of the complex image amplitude. Averaging is implemented by multilooking, as is common in many SAR imagery applications.

Other quantitative measures follow from the Stokes parameters. They are:

$$m_L = \frac{\sqrt{S_1^2 + S_3^2}}{S_1} \qquad m_C = \frac{S_4}{S_1} \qquad \mu_C = \frac{S_1 - S_4}{S_1 + S_4} \qquad \mu_L = \frac{S_1 - S_2}{S_1 + S_2}$$

Here, m_L is the degree of linear polarization, m_C is the degree of circular polarization, μ_C is the circular polarization ratio (CPR), and μ_L is the linear polarization ratio. In particular, μ_C has been used to characterize volume scattering in the reflected imagery indicative of lunar ice [2]-[5]. Figures 4 and 5 show the S_1 Stokes parameter and μ_C for signals over from the low-power Arecibo-to-LRO bistatic collection? respectively.

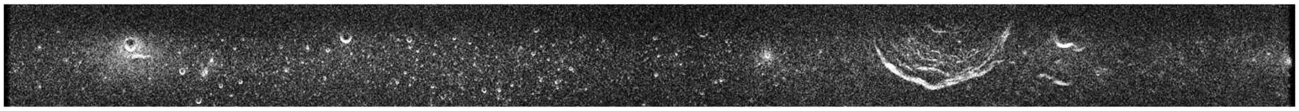

Figure 4. The S1 Stokes parameter bistatic SAR image for a 400-km north-to-south swath of the moon. The large crater on the right is Hansteen crater.

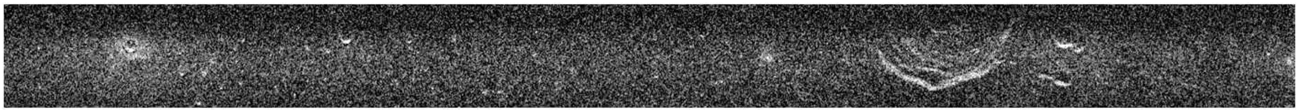

Figure 5. The CPR parameter bistatic SAR image for collection described above. CPR measure are scaled from 0 (dark) to 3.0 (bright).

6. CONCLUSIONS

We have demonstrated that bistatic SAR imaging of the lunar surface is viable when we employ a fixed earth-based transmitter with a radiated power of 35 watts and a lunar orbiter for the receiver. The polarimatric bistatic images can be employed to produce a parameter, CPR, that may be able to help discern the probability of lunar ice at the bottom of various craters that are never illuminated by the sun. Future collections will confirm or deny this possibility.

7. ACKNOWLEDGMENTS

Sandia National Laboratories is a multi-program laboratory managed and operated by Sandia Corporation, a wholly owned subsidiary of Lockheed Martin Corporation, for the U.S. Department of Energy's National Nuclear Security Administration under contract DE-AC04-94AL85000.

.

REFERENCES

[1] Arnold, J. R., “Ice in the lunar polar regions,” J. of Geophys. Res. 84(NB10), 5659-5668 (1979).

[2] Nozette, S., Spudis, P. D.., Robinson, M. S., Bussey, D. B. J., Lichtenberg, C. , and Bonner, R., “Integration of lunar polar remote-sensing data sets: Evidence for ice at the lunar south pole,”, J. of Geophys. Res. - Planets 106(E10), 23253-23266 (2001).

[3] Campbell, D. B., Campbell, B. A., Carter, L. M., Margot, J. L., and Stacy, N. J. S, “No evidence for thick deposits of ice at the lunar south pole,” Nature 443(7113), 835-837 (2006).

[4] Nozette, S., Spudis, P., Bussey, B., Jensen R., Raney, K., Winters, H., Lichtenberg, C. L., Marinelli, W., Crusan, J. Gates, M. and Robinson, M., “The Lunar Reconnaissance Orbiter Miniature Radio Frequency (Mini-RF) Technology Demonstration,” Space Science Reviews 150(1), 284-302 (2010).

[5] Spudis, P. D., Bussey, D. B. J., Baloga, S. M., Butler, B. J., Carl, D. Carter, L. M., *et. al.* , “Initial results for the north pole of the Moon from Mini-SAR, Chandrayaan-1 mission”, Geophys. Res. Letters 37, L06204 (2010).

[6] Jakowatz, C. V. Jr., Wahl, D. E., and Yocky, D. A., “A beamforming algorithm for bistatic SAR image formation,” Proc. SPIE 7699, 769902 (2010).

[7] Raney, R. K., “Dual-polarized SAR and Stokes Parameters,” IEEE Geosci. and Remote Sens. Letters 3(3), (2006).